

Subscriber access provided by UNIV OF WISCONSIN - MADISON

Interface Components: Nanoparticles, Colloids, Emulsions, Surfactants, Proteins, Polymers

Synthesis and Degradation of Cadmium-Free InP and InPZn/ZnS Quantum Dots in Solution

Richard P. Brown, Miranda J. Gallagher, D. Howard Fairbrother, and Zeev Rosenzweig

Langmuir, Just Accepted Manuscript • Publication Date (Web): 23 Oct 2018

Downloaded from http://pubs.acs.org on October 23, 2018

Just Accepted

"Just Accepted" manuscripts have been peer-reviewed and accepted for publication. They are posted online prior to technical editing, formatting for publication and author proofing. The American Chemical Society provides "Just Accepted" as a service to the research community to expedite the dissemination of scientific material as soon as possible after acceptance. "Just Accepted" manuscripts appear in full in PDF format accompanied by an HTML abstract. "Just Accepted" manuscripts have been fully peer reviewed, but should not be considered the official version of record. They are citable by the Digital Object Identifier (DOI®). "Just Accepted" is an optional service offered to authors. Therefore, the "Just Accepted" Web site may not include all articles that will be published in the journal. After a manuscript is technically edited and formatted, it will be removed from the "Just Accepted" Web site and published as an ASAP article. Note that technical editing may introduce minor changes to the manuscript text and/or graphics which could affect content, and all legal disclaimers and ethical guidelines that apply to the journal pertain. ACS cannot be held responsible for errors or consequences arising from the use of information contained in these "Just Accepted" manuscripts.



Synthesis and Degradation of Cadmium-Free InP and InPZn/ZnS Quantum Dots in Solution

Richard P. Brown¹, Miranda J. Gallagher², D. Howard Fairbrother² and Zeev Rosenzweig*¹

¹Department of Chemistry and Biochemistry, University of Maryland Baltimore County, Baltimore, MD 21250

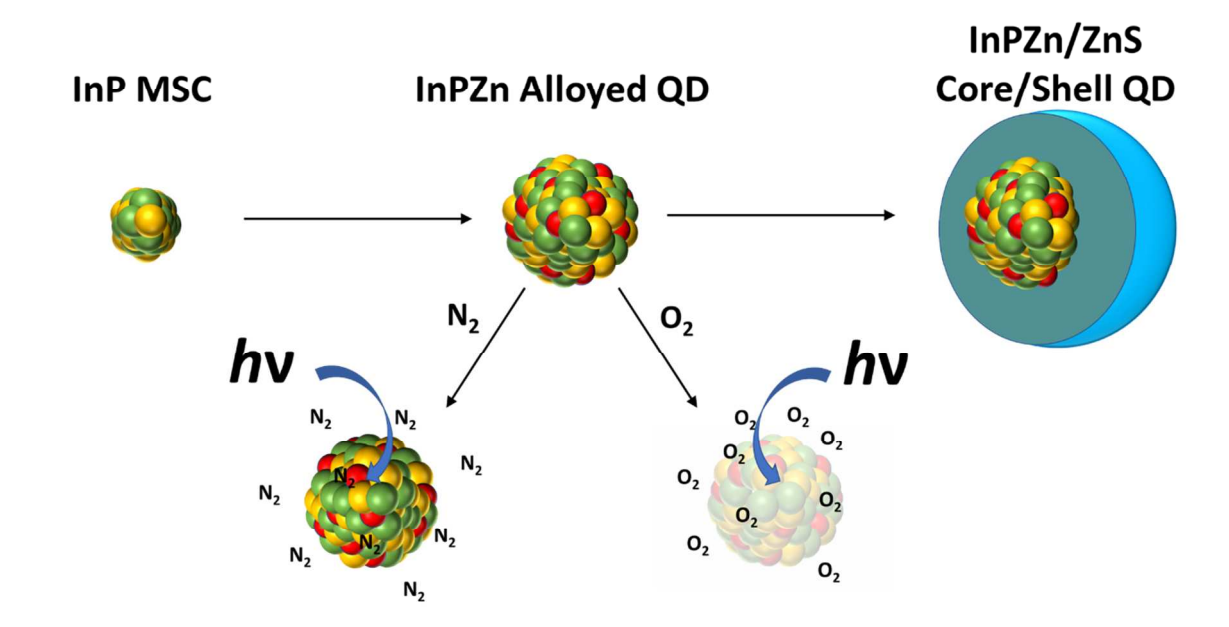
²Department of Chemistry, Johns Hopkins University, Baltimore, MD 21218

^{*}Email of corresponding author – <u>zrosenzw@umbc.edu</u>

ABSTRACT

This study advances the chemical research community toward the goal of replacing toxic cadmium-containing quantum dots (QD) with environmentally benign InP QD. The InP QD synthesis uniquely combines the previously reported use of InP magic-sized clusters (MSCs) as a single-source precursor for indium and phosphorous to form InP QD, with zinc incorporation and subsequent ZnS shelling, to form InPZn/ZnS QD with comparable luminescence properties to commonly used cadmium-containing luminescent OD. The resulting InPZn/ZnS OD have an emission quantum yield of about 50% across a broad range of emission peak wavelengths and emission peaks averaging 50 nm in Full Width at half Maximum (FWHM). The emission peak wavelength can be easily tuned by varying the Zn:In ratio in the reaction mixture. The strategy of using zinc stearate to tune the emission properties is advantageous since it does not lead to a loss of emission quantum yield or emission peak broadening. While the initial optical properties of InP and InPZn/ZnS QD are promising, thermal stability measurements of InPZn QD show significant degradation in the absence of a shell compared to the CdSe QD particularly at elevated temperature in the presence of oxygen, which is indicative of thermal oxidation. There is no significant difference in the degradation rate of InP QD made from molecular precursors and from MSCs. Additionally, the emission intensity and quantum yield of InPZn/ZnS OD decrease significantly when purified and diluted in organic solvents under ambient conditions compared to CdSe/ZnS QD. This indicates instability of the ZnS shell when prepared by common literature methods. This must be improved to realize high quality, robust Cd-free QD with the capability to replace CdSe QD in QD technologies.

TOC Graphics



INTRODUCTION

InP/ZnS and InPZnS/ZnS core/shell and alloy/shell quantum dots (QD) have been recently proposed as a viable, cadmium-free alternative to cadmium-containing QD such as CdS/ZnS, CdSe/ZnS, and CdTe/CdSe/ZnS QD. 1-5 Historically, a major challenge for InP QD synthesis lies in the need to replace highly reactive, pyrophoric phosphorous precursors like tris(trimethylsilyl)phosphine [P(TMS)₃] with safer and more stable precursors. In addition to posing significant safety concerns, the use of highly reactive molecular precursors leads to heterogeneous crystal growth, broad InP QD size distribution, and broad emission peaks.⁶ Another challenge lies with the inherently low photoluminescence quantum yield of InP QD. The low quantum yield of about 1% has been attributed to non-radiative exciton relaxation pathways associated with unsaturated "dangling" phosphorous bonds. One approach to increase the photoluminescence quantum yield involves coating the InP QD cores with a higher energy band gap material such as ZnS. The ZnS shell passivates surface defects, confines excitons, prevents core oxidation, and significantly increases the photoluminescence quantum yield of InP/ZnS core/shell OD to about 40%. 9, 10 Another approach has been to grow an interfacial layer between the core and the shell to better passivate defects and to enable the formation of a more complete shell. This approach was reported to increase the photoluminescence quantum yield of InPZnS/ZnS QD up to 70%. However, the photoluminescence quantum yield of QD that were prepared using this technique varied greatly with emission wavelength. The resulting OD were heterogeneous in size, which resulted in broad emission peaks.⁴ Other studies have attempted to narrow the size distribution of InP QD by replacing the highly reactive phosphorous molecular precursors with less reactive molecular precursors like tris(trimethyl)germanium phosphide, triarylsilylphosphine, and aminophosphine. 11-13 This resulted in some narrowing of the size distribution and emission peaks but did not lead to significant improvement in the photoluminescence quantum yield of InP/ZnS QD. Furthermore, most strategies for tuning the optical properties result in inconsistent QD properties and a need to optimize many reaction parameters. Table 1 summarizes how FWHM values can change depending on emission color. 1, 4, ^{14, 15} Recently, Lee and coworkers published a technique for making InP-based core/shell QD with peaks less than 40 nm FWHM. 15 There results are quite impressive, but rely on a much longer reaction time of around 5 hours and a complicated setup, which highlight the need for

simple, highly reproducible methods for making high quality InP-based QD. Studies by Cossairt and co-workers demonstrated the possibility of forming monodisperse InP QD using magic-sized clusters (MSCs) as the source of both phosphorus and indium.⁶ MSCs are obtained in a wide range of nanocrystals and their presence plays a significant role in many crystal growth mechanisms.¹⁶⁻¹⁸ Cossairt and coworkers discovered that InP MSCs could be synthesized in gram quantities from P(TMS)₃ and indium myristate (MA) at a relatively low temperature, and used as a single-source precursor for the synthesis of InP QD.⁶ They also obtained the crystal structure of phenyl acetate (PA) coated InP MSCs using x-ray crystallography, allowing them to determine the core structure and atomic formula of InP MSCs to be In₃₇P₂₀.¹⁹

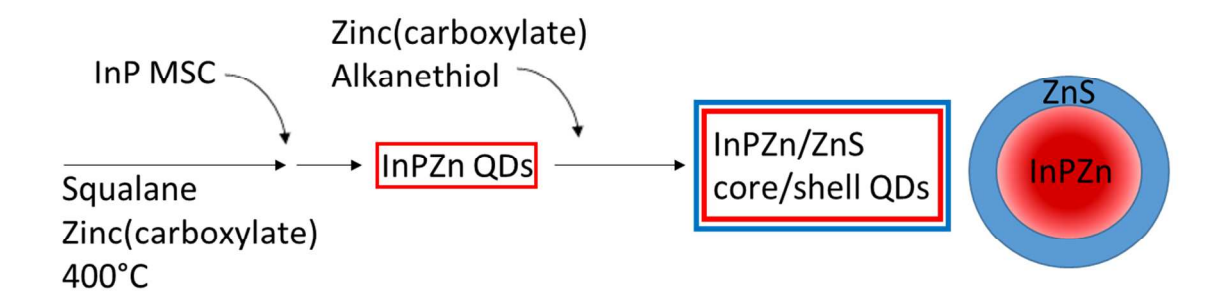
Reference:	~500nm	~525nm	~550nm	~575nm	~600nm
Mutlugun (2016)	47nm	45nm	67nm	94nm	90nm
Houtepen (2016)	X	Х	69nm	79nm	70nm
Reiss (2008)	40nm	42nm	50nm	56nm	58nm
This study (2018)	47nm	50nm	52nm	50nm	Х
Lee (2018)	X	37nm	36nm	36nm	37nm

Table 1 – Emission peak widths from a selection of recent InP/ZnS QD publications given as FWHM. The values are categorized at the peak's λ_{max} within 25nm of the λ given in the top row. X's indicate that this wavelength was not provided in the original experimenter's data set.

In this paper we demonstrate a simple and scalable synthesis method to form highly luminescent InPZn/ZnS QD from non-pyrophoric InP(MA) MSCs and zinc stearate. Including zinc stearate in the reaction mixture provides an easy and reproducible method for controlling the size and bandgap of the resulting QD. Coating these InPZn QD with a ZnS shell is performed without any purification steps to produce strongly luminescent core/shell InPZn/ZnS QD with high photoluminescence quantum yield, and decently narrow and tunable emission peaks. Unique to this strategy is the maintenance of high photoluminescence quantum yield and emission peak width over a broad range of emission wavelengths. Although these numbers are not "record breaking", the simplicity and speed of this strategy provide significant value to the

field. Additionally, this synthesis approach eliminates the use of pyrophoric precursors in the high temperature QD synthesis and leads to the formation of luminescent QD with optical properties rivaling those of the widely used CdSe/ZnS QD. Employing InP MSCs as a single source reactant for indium and phosphorus in the synthesis of luminescent InPZn/ZnS QD alleviates significant safety concerns, because the exposure to P(TMS)₃ is minimized to a single, low temperature procedure used to form the InP MSCs in high yield. The resulting InP MSCs are non-pyrophoric and could be used to synthesize >100 samples of highly luminescent InPZn/ZnS QD in milligram quantities from the same batch of InP MSCs. The use of InP MSCs as a precursor leads to improved consistency and reproducibility of the InPZn/ZnS OD structure and properties by greatly simplifying their synthesis (Scheme 1). This study also evaluates the chemical and thermal stability of InPZn QD that are made from InP MSCs and compares them to InP and CdSe QD made from molecular precursors. Long term chemical and thermal stability of luminescent QD is imperative to the functionality of QD based consumer electronic devices, which often operate at elevated temperatures. Methods to improve stability often rely on thick silica coatings²⁰ or embedding the QD into polymers.²¹ These strategies, however, do not apply to small, colloidal QD that are intended for biological imaging and sensing applications. A limited number of studies have been conducted to evaluate the chemical and thermal stability of colloidal InP OD towards photoinduced or thermally induces oxidation. ^{22, 23} Typically, these experiments monitor core/shell OD photoluminescence over time under constant illumination. More insight can be gained however by studies such as those performed by Houtepen and coworkers who evaluated various InP-based QD alloyed with Ga and Zn under constant illumination, and showed that certain multi-shell configurations provide superior stability.²⁴ In a different study, Zhang and coworkers showed that InPZn QD made from PH₃ (P precursor) and zinc stearate increased in photoluminescence and their absorption spectrum remained stable for over 30 days when the QD were suspended in hexane and stored in the dark.²⁵ They attributed the photoluminescence enhancement to oxidation of P, which resulted in the elimination of dangling phosphorous bonds. The limited number of studies did not look systematically at the effects of heat and oxygen on core degradation.

$Scheme\ 1-Synthesis\ of\ InPZn\ and\ InPZn/ZnS\ Quantum\ Dots\ from\ InP\ Magic\ Sized$ Clusters



MATERIALS AND METHODS

Reagents - Tris(trimethylsilyl)phosphine, $P(TMS)_3$, ($\geq 98\%$) was purchased from Strem chemicals and hexamethyldisilathiane, S(TMS)₂, (synthesis grade) was purchased from Sigma-Aldrich. Both were handled in a nitrogen filled glovebox. Zinc formate (98%) and 1dodecylphosphonic acid (95%) were purchased from VWR. All other chemicals were purchased from Sigma-Aldrich. Indium(III) acetate (99.99% trace metal basis), Myristic acid (≥99%), zinc stearate (purum grade), cadmium acetylacetonate (≥99.9% trace metals basis), tetradecylphosphonic acid (97%), hexadecylamine (98%) and oleylamine (98%) were used as received. Anhydrous trioctylphosphine (97%) was stored in the glovebox. 1-dodecanthiol and oleic acid (90%) were degassed and stored in the glovebox. Squalane (96%) and 1-octadecene (90%) were dried over CaH₂, distilled and stored over molecular sieves in the glovebox. Toluene (99.8%), pentane (\geq 99%) and acetonitrile (99.8%) that were used for synthesis were all anhydrous grade and stored over molecular sieves in the glovebox. All air-sensitive manipulations were performed under inert conditions, either in a glovebox or on a Schlenk line in the fume hood. The Schlenk line was supplied by high purity N₂ which passed through a cylinder filled with drierite. Solvents used for the degradation studies were ACS grade and used without further purification.

Extreme caution should be taken when working with P(TMS)₃. It is pyrophoric when exposed to air and phosphides, in general, can form PH₃, an extremely toxic gas when exposed to acidic protons, including water. Small quantities of P(TMS)₃ residue should be carefully quenched with bleach in a well-ventilated fume hood.

Synthesis of myristate-coated InP magic-sized clusters (InP(MA) MSCs) - InP(MA) MSCs were made according to a scaled-up version of Cossart's method. We typically used the entire ampule of P(TMS₃) from the chemical supplier so as to not leave unused pyrophoric reagents in the lab. Since heterogeneous thermal mixing is less of a concern with equilibrium reactions, we anticipate that this reaction could be scaled to much larger, industrial sized productions. The reaction was carried out in a 3-necked flask, which was equipped with a thermocouple, condenser, septum and stir bar. (The following amounts should be adjusted after determining the

exact amount of P(TMS)₃ in the supplied ampule). A typical flask contained indium acetate (9.5 mmoles) and myristic acid (34.4 mmoles). The reaction mixture was then degassed (vac/fill multiple times) and heated under nitrogen until all reactants were melted and well mixed. Vacuum was carefully applied, trying to avoid splattering while heating to 100°C. The mixture was left overnight under vacuum at 100°C to form indium myristate. The next day, the system was backfilled with N2 and dry toluene (40mL) was added to the indium myristate and heated to 110°C. P(TMS)₃ (4mmoles) was dispersed in dry toluene (20mL) in a syringe equipped with a needle in the glovebox. After capping with a septum, the syringe was transferred to the fume hood and added to the In(MA) mixture. The reaction was monitored by taking samples for UV-Vis absorption spectroscopy measurements at various time intervals. Almost immediately, the color changed from clear to yellow. After about 45-60 minutes, the excitonic peak was fully defined and no longer changed, showing evidence of reaching completion. After cooling, the toluene was removed by applying vacuum in the Schlenk line, and the crude product was transferred to the glovebox for purification, while carefully avoiding the introduction of air. Cooling the toluene on ice and carefully using a room temperature water bath to alternate warming/cooling made evaporation much easier to control on the high vacuum levels of our Schlenk line. In the glovebox, small portions of dry toluene were used to transfer and dissolve the crude MSCs to airtight centrifuge tubes. The sealed tubes were removed from the glovebox for centrifugation. After each centrifugation, the tubes were returned to the glove box for all manipulations. An initial centrifugation (10k x G, 15 minutes) was used to remove insoluble material and supernatant was transferred to a clean, centrifuge tube to be precipitated with dry acetonitrile. After 3-5 precipitation/centrifugation/resuspension washes (10k x G, 5 minutes) with dry toluene and dry acetonitrile under N₂, dry pentane was used to dissolve and transfer the final MSC pellet to a clean scintillation vial. Careful evaporation of the pentane yielded pure InP(MA) MSCs as a waxy, bright yellow solid. Later dissolution into room temperature squalane produced a completely translucent yellow solution. If MSCs were carefully protected from air during the washing procedure, the UV-Vis absorption spectrum remained unchanged after the washing procedure.

Synthesis InPZn alloyed core quantum dots from magic-sized clusters (InPZn MSC QD core) (Scheme 1) - A typical synthesis to form InPZn (25% Zn:In) MSC QD cores is as follows.

A 3-necked round bottom flask equipped with a thermocouple, condenser and glass-coated stir bar was attached to the Schlenk line. 56 µmoles zinc stearate and 7.5mL dry squalane were added and the flask was plugged with a rubber septum. With stirring, the flask was evacuated and filled with nitrogen multiple times and heated under vacuum until the squalane almost began to boil, whereupon the flask was filled with nitrogen and the TC was set to around 200°C. Meanwhile, a syringe of 100mg of InP MSCs in 2mL of dry squalane was prepared in a glovebox and capped with a septum to allow for transfer outside the glovebox. When everything was ready, the TC was set to a very high temperature (around 600°C) to allow for rapid heating. The InP MSC solution was swiftly injected into the hot zinc stearate solution when the temperature reached above 395°C. Because of the room temperature injection, the reaction temperature would drop to around 360°C and climb to about 370°C in about 1 minute. At 1 minute, the mantle was removed, and the extremely hot flask was carefully lowered into a room temperature silicone oil bath to cool quickly. A portion could be removed and stored in the glovebox as InPZn MSC QD cores for future analysis.

Synthesis of InPZn/ZnS MSC core/shell QD - Once at room temperature an additional 200 umoles of zinc stearate was added to the above reaction mixture under nitrogen flow. The mixture was degassed multiple times and heated to 230°C under N₂. After 3 hours and without cooling, 200uL of [1M] 1-dodecanthiol in dry squalane was added over 15 minutes by a syringe pump. After 1 hr at 230°C to allow for ZnS shell to grow, the reaction mixture was cooled, transferred to a 20-mL glass scintillation vial and flushed with nitrogen before storing. Core/shell QD are significantly more resistant to water/oxygen degradation than InP MSCs or even InP QD cores. The core/shell QD can be handled easily on the bench top using standard solvents. Although any effort to exclude light and oxygen will help maintain their desired properties, extreme measures are not necessary. Storing at room temperature in the dark maintains sufficiently bright QD, but immediate transfer to the glovebox appeared to maintain higher luminescence stability when InPZn/ZnS QD solutions were stored for long periods. QD purification was realized by first diluting the InPZn/ZnS QD in toluene and removing insoluble precipitates by centrifugation. We then added a small amount of ethyl acetate as a co-solvent (for the viscous squalane) and precipitated the QD with acetonitrile. Initial precipitation by centrifugation yields an oily liquid pellet. Further washing cycles which include resuspension in

toluene, precipitation with acetonitrile and centrifugation, yield compact QD pellets that disperse fully in non-polar solvents

Synthesis of InPZn/ZnS MSC QD with Varying Emission Peak wavelength - The size and emission peak of InPZn/ZnS MSC QD is affected by many parameters including InP MSC concentration, reaction temperature, and injection volume (which affects temperature drop after injection). However, we found that increasing the concentration of zinc stearate, while keeping all other parameters constant, enable tuning the λ_{max} of the emission peak to the blue while maintaining narrow emission peak widths (FWHM). See (table 2) for suggested concentrations for targeting specific wavelengths. All concentrations are given as a percent zinc stearate to total indium. %50 means that for 100mg InP(MA) MSCs = 225umoles indium and therefore 112.5umoles of zinc stearate should be used. Shelling procedure is identical for each size.

Synthesis of CdSe and CdSe/ZnS core and core/shell QD - CdSe core and CdSe/ZnS core/shell QD were made according to the method published by Mulvaney, with slight modifications²⁶.

CdSe core QD - In a nitrogen-filled glovebox, selenium powder (4.2mmol) was dissolved in trioctylphospine (5mL) by stirring in a vial for about 1 hour. In a 50mL 3-neck flask, a magnetic stir bar, cadmium acetylacetonate (1.0mmol), hexadecylamine (20.7mmol), tetradecylphosphonic acid (2.1mmol) and trioctylphosphine (10mL) were combined and the flask was equipped with a septum, thermocouple and condenser. This mixture was degassed under multiple cycles of vacuum/purge on a nitrogen filled Schlenk line. Then the solution was heated to 100C under vacuum for > 30 minutes. After backfilling with N₂, the solution was heated to 250°C for 1 hour to dissolve the cadmium precursor. The mixture was allowed to cool to 120-100°C and vacuum was reapplied for 30 minutes to remove any volatile side products. Finally, the reaction flask was filled with nitrogen and heated to 320°C where the mantle was set to 270°C. When the temperature dropped to 300°C, the TOP-Se solution from the glovebox was swiftly injected into the hot reaction mixture. The temperature dropped to 260°C and crystal growth occurred up to 270°C for 5 minutes after injection, whereupon the reaction mixture was cooled quickly and allowed to anneal at 80°C for 30 minutes.

CdSe/ZnS core/shell QD - 6.5mL of room temperature CdSe crude reaction mixture was mixed with butanol (4mL), vortexed and centrifuged (3K x G for 5 minutes). The supernatant was discarded, and the pellet was resuspended in CHCl₃ (5mL). The QD were centrifuged again (3K x G for 5 minutes). The QD layer was removed to a clean vial and 4:1 acetone/methanol (about 5mL) were added to precipitate OD. After a final centrifugation (3K x G for 5 minutes), the OD pellet was resuspended in hexane (5mL). UV-Vis absorbance was used to determine concentration [25uM] (4.8mL) = 0.12umoles. $\varepsilon_{532} = 172,284 \text{ L mole}^{-1} \text{ cm}^{-1}$ was estimated using Mulvaney's equation relating excitonic peak position to OD size and molar extinction coefficient. 26 Zinc and sulphur precursor solutions were prepared in a glovebox so that syringes could be used to alternate injecting the cation/anion shell component to grow ZnS shell layer by layer. These solutions consisted of [0.05M] zinc formate in oleylamine and a [0.1M] hexamethyldisilathiane (S(TMS₂) in trioctylphosphine. The solutions were kept in vials with stirbars in the glove box until each injection was needed. The sulfur solution was capped with a septum to contain unpleasant sulfur smell as best as possible. Purified CdSe cores (0.12 μmoles) Φ_{PI} 16% were added to a 50mL 3-neck flask that contained a stir bar, octadecene (6mL), oleylamine (6mL), trioctylphosphine (4mL) and 1-dodecylphosphonic acid (40µmoles). After attaching a condenser, septum and thermocouple, the flask was evacuated to remove air and hexane for the QD purification. The mixture was degassed with multiple rounds of vacuum/purging with nitrogen and heated to 80°C under vacuum for >1 hour and then filled with nitrogen. For the first ZnS layer, Zn-oleylamine (606 µL)[0.05M] was injected into the CdSe core solution over 15 minutes by syringe pump at 80°C and heated. After the temperature reached 160°C, S(TMS)₂ (303 µL)[0.1M] was injected over 15 minutes and allowed to anneal for another 30minutes. Φ_{PL} increased to 52%. The second ZnS layer was grown by injecting Znoleylamine (866 μL)[0.05M] at 160°C over 15 minutes and then heated to 180°C where S(TMS)₂ (433 μ L)[0.1M] was injected. The ZnS layer annealed for 30 minutes. Φ_{PL} was 47%. The third layer of ZnS was grown similarly, but used Zn-oleyamine (1170 µL) [0.05M] and S(TMS)₂ (586 μL)[0.1M] at 180°C. Φ_{PL} was 53%. Oleic acid (0.5mL) was added slowly and core/shell QD allowed to anneal at 200°C for 1 hour.

Synthesis of InPZnS alloyed core and InPZnS/ZnS core/shell quantum dots from molecular precursors (InPZnS MP QD) and (InPZnS/ZnS MP QD) - InPZnS MP alloyed core and InPZnS/ZnS MP alloyed core/shell QD were made according to established literature procedures with minor adjustments. The phosphorous precursor was prepared in a nitrogen filled glovebox by dispersing P(TMS)₃ (0.1mmoles) in octadecene (2mL), drawn into a syringe, capped and left in the glovebox antechamber until ready for injection. Indium acetate (0.2mmoles), myristic acid (0.86mmoles) and octadecene (16mL) were loaded into a 50mL 3-neck flask equipped with a stir bar, a condenser, a septum and a thermocouple. The vessel was degassed by multiple vacuum/purge cycles and heated at 100°C under vacuum for >1.5hrs to form indium myristate. The mixture was cooled to room temperature and zinc stearate (0.2mmol) and 1-dodecanthiol (0.05mmoles) were added. The mixture was again degassed and heated under vacuum to 50°C at which point it was put under nitrogen for continued heating. When ready to inject the phosphorous solution, the heating mantle was set to a high setting (>300°C). At 220°C, the P(TMS)₃ solution was quickly injected. The temperature dropped to 210°C and rose quickly to 285°C. The time from injection to reaching 280°C was about 10 minutes. Crystal growth was allowed to continue for an additional 10 minutes (280-285°C). The reaction was terminated by cooling quickly to room temperature. 1mL of the InPZnS MP QD cores were removed for characterization and degradation studies. Shelling InPZnS MP cores to form InPZnS/ZnS MP core/shell OD was performed by adding zinc stearate (0.375mmol) to the crude room temperature InPZnS MP cores described above without purification. The mixture was degassed and heated under vacuum to 100°C and backfilled with nitrogen. The flask was kept at 230°C for 3 hrs, at which point, 1-dodecanethiol (0.75mmol) in octadecene (2mL) was slowly injected into the mixture. The ZnS shell was allowed to grow at 230°C for 1 hour. The InPZnS/ZnS MP QD were stored in a vial away from light. They can be purified similarly to other hydrophobic QD using hexane, acetone and centrifugation to selectively disperse, flocculate and separate insoluble QD or impurities from soluble ones.

InP MSCs and InPZn QD Characterization - The optical properties of InP MSCs, InPZn MSC core QD, and InPZn/ZnS MSC core/shell QD were determined with a Thermo Scientific Evolution 201 UV-Vis spectrophotometer (excitonic peak) and a PTI Quantum Master 400 fluorimeter (Φ_{PL} , peak position (λ_{max}) and peak full width at half maximum (FWHM)). Φ_{PL} was

determined using a K-Sphere Petite integrating sphere using a 375nm excitation wavelength, 1.35nm excitation slits and 0.5 nm emission slits. Crude reaction mixtures were diluted in hexane, centrifuged and translucent QD supernatant was transferred to clean vial before optical measurements were performed. Final concentrations were adjusted to less than 0.1 absorbance at excitation λ_{375} before measuring photoluminescence spectra/ Φ_{PL} . Standard deviation is given for each QD batch (**Table 2**) determined by 3 purifications and measurements of each crude reaction mixture on 3 different days.

ICP-MS Measurements of InP(MA) MSCs - ICP-MS measurements were conducted to determine the precise amounts of In(III) in the MSC batches to calculate the molar extinction coefficient for the MSCs. Different batches of InP(MA) MSCs were used to determine [In $^{3+}$] in InP MSC samples after acid digestion (see SI for a detailed example of calculation). InP MSCs were digested in a 70% HNO $_3$ solution. The digested samples were diluted to solutions with In(III) concentrations between 1ppb and 1ppm. We used a molecular formula of In $_{37}$ P $_{20}$ (O $_2$ H $_{17}$ C $_{14}$) $_{51}$ for our myristate coated InP MSCs. This was based on the molecular formula of phenyl acetate coated InP MSC In $_{37}$ P $_{20}$ previously reported by Cossairt and coworkers 2 while accounting for changes in ligand molecular weight. This formula was used to estimate In(III) concentration of these solutions to contain amounts that fell within the ICP-MS instrument's best detection window (1ppm-1ppb). Standard curves were made from diluting indium (1ug/mL Indium in 2% HNO $_3$ Perkin Elmer Pure Plus #N9304234) to six concentrations between 1ppb and 1ppm in 2% HNO $_3$. The digested samples were compared to the standard curve (R 2 =0.9938) to give In(III) content using the In 114 isotope. All samples and standards were made to 2% HNO $_3$ concentration and used MS grade reagents.

XPS analysis of InP MSCs - InP MSCs were smeared onto a silicon chip and analyzed by X-ray photoelectron spectroscopy (XPS) on a Phi 5600 (P_{base} <5x10⁻⁹torr) with a Mg K α X-ray source (1253.6eV, 15KV, 300 W); photoelectrons were detected at a pass energy of 58.7eV with a scan rate of 0.125 eV/step. Casa XPS software was used to calibrate all spectra to the C (1s) to the hydrocarbon group at 248.8 eV, fit each peak with a Tougaard background and fit the P (2p) peak to calculate atomic percentages.

Degradation studies - OD cores (CdSe, InPZnS MP and InPZn MSC) were stored in a nitrogen filled glovebox. Core/shell QD (CdSe/ZnS, InPZnS/ZnS MP, InPZn/ZnS MSC) were stored in a dark drawer at room temperature. InPZn MSC QD (25% Zn: In) was the QD core used for all stability studies to represent the QD made from magic-sized clusters. 100ul of stock QD [10-90uM] were dispersed in 1ml toluene and centrifuged at 4,000 x G for 10 minutes to remove insoluble material leftover from synthesis. The supernatant was passed through a 0.45µm nylon syringe filter, rinsed and diluted with toluene to give absorbance values around 0.03 at the lowest energy excitonic peak (~500-550nm). Glass cuvettes were selected that gave similar absorbances using a dedicated toluene-filled blank cuvette. All samples were kept in these matched glass cuvettes with a small stir bar and PTFE-lined screw top or a rubber septum top for the duration of the degradation experiment. Samples that are described as being kept in the dark were stored in a drawer at room temperature. All other samples were kept in the hood, exposed to ambient room light and sunlight (both oscillating between day and night). For degradation experiments under nitrogen, nitrogen was bubbled through the QD solution and slight positive nitrogen pressure was provided through a needle in the septum-capped cuvette during the experiment. For the heated samples, some toluene was lost over the course of the experiment. This solvent level was returned by carefully adding nitrogen infused or standard benchtop toluene (as appropriate) before each measurement to avoid any absorbance changes due to concentration. Nitrogen was bubbled through the samples for 15 minutes before returning to heat anytime the nitrogen samples were removed from the Schlenk line. Before every measurement, the samples were allowed to cool to room temperature.

RESULTS AND DISCUSSION

Characterization of InP MSCs - Structural and spectroscopic characterization of InP(MA) MSCs is provided in **Figure 1**. High resolution transmission electron microscopy (HRTEM) images of InP MSCs are difficult to obtain due to the small size (1-2 nm) and low z contrast between InP MSCs and the carbon film of the TEM grids. Poorly resolved nanoparticles can be seen in HRTEM images (see supporting information Figure S1). Significantly higher contrast is obtained by using Scanning Transmission Electron Microscopy (STEM), which is equipped with a High-Angle Annular Dark-Field (HAADF) imaging detector. Figure 1a shows a representative STEM image of InP(MA) MSCs. A histogram showing the size distribution of the MSCs is shown in the insert(details on instrument and analysis are given in supporting information). The use of STEM enables, for the first-time, visual observation and quantitative image analysis which reveals that the InP MSCs have an average diameter of 1.3 nm with a standard deviation (SD) = 0.37 nm. The polydispersity in the MSCs size, is attributed to the low signal/background ratio in STEM images of InP MSCs in this size range, and to the asymmetric crystal structure of InP MSCs. 19 UV-Vis measurements (**Figure 1b**) show that the InP(MA) MSCs have a welldefined excitonic peak at 384 nm, with a small shoulder at 420nm, which was attributed in a previous study to two independent optical transitions as calculated using time-dependent density functional theory calculations.⁶ InP(MA) MSCs samples that had been exposed to air will show a poorly defined, broad peak (not shown), indicating chemical/structural degradation. This oxidative degradation is accompanied by the appearance of a phosphate peak in the XPS data (data not shown). Interestingly, even MSC samples with poorly defined peaks could be used as a single source precursor to yield high quality InP QD. This result indicates significant structural rearrangement at the high temperatures used to form InP QD from InP MSCs versus a purely agglomeration growth mechanism.

XPS analysis of InP(MA) MSCs - X-ray photoelectron spectroscopy (XPS) spectra of InP(MA) MSCs shown in **Figure 1C**, confirms the formation of indium phosphide with an In(3d_{5/2}) binding energy at 444.7eV, within the average of eight NIST database values of 444.6 \pm 0.6eV. The indium (3d_{3/2}) and (3d_{5/2}) peaks show a typical spin-orbit splitting of 7.5 eV. The lack of additional peaks, asymmetry or broadening indicates well-passivated indium with no other

indium-containing surface species present. In the P(2p) region, the single peak at 128.6 eV is consistent with literature values for InP at 128.6 ± 0.6 eV. The absence of any oxidized phosphorous atoms (binding energy ≈ 135 eV) confirms the effectiveness of ligand passivation towards phosphorous oxidation. The small peak to the low binding energy side of the P(2p) peak is due to an In(4s) transition. XPS spectral analysis of the In($3d_{5/2}$) and P(2p), which includes consideration of differences in relative sensitivity factors as well as differences in electron transmission and escape depths, reveals an atomic composition ratio of 72% In : 28% P . Within the instrumental error of XPS measurements, this ratio agrees well with the core crystal structure of In₃₇P₂₀ for InP MSCs which was proposed by Cossairt and coworkers (65%:35% In:P ratio) for InP(PA) MSCs¹⁷. The C(1s) region shows a dominant peak at 284.8 eV due to CH₂/CH₃ carbon atoms with a smaller carboxyl peak at 288.4eV. The presence of these two features as well as their intensity ratio (14:1 CH₂/CH₃:COO⁻ ratio) is consistent with the presence of the myristate ligand (CH \square (CH \square) \square COO⁻). Overall, the XPS measurements indicate the formation of pure InP(MA) MSCs.

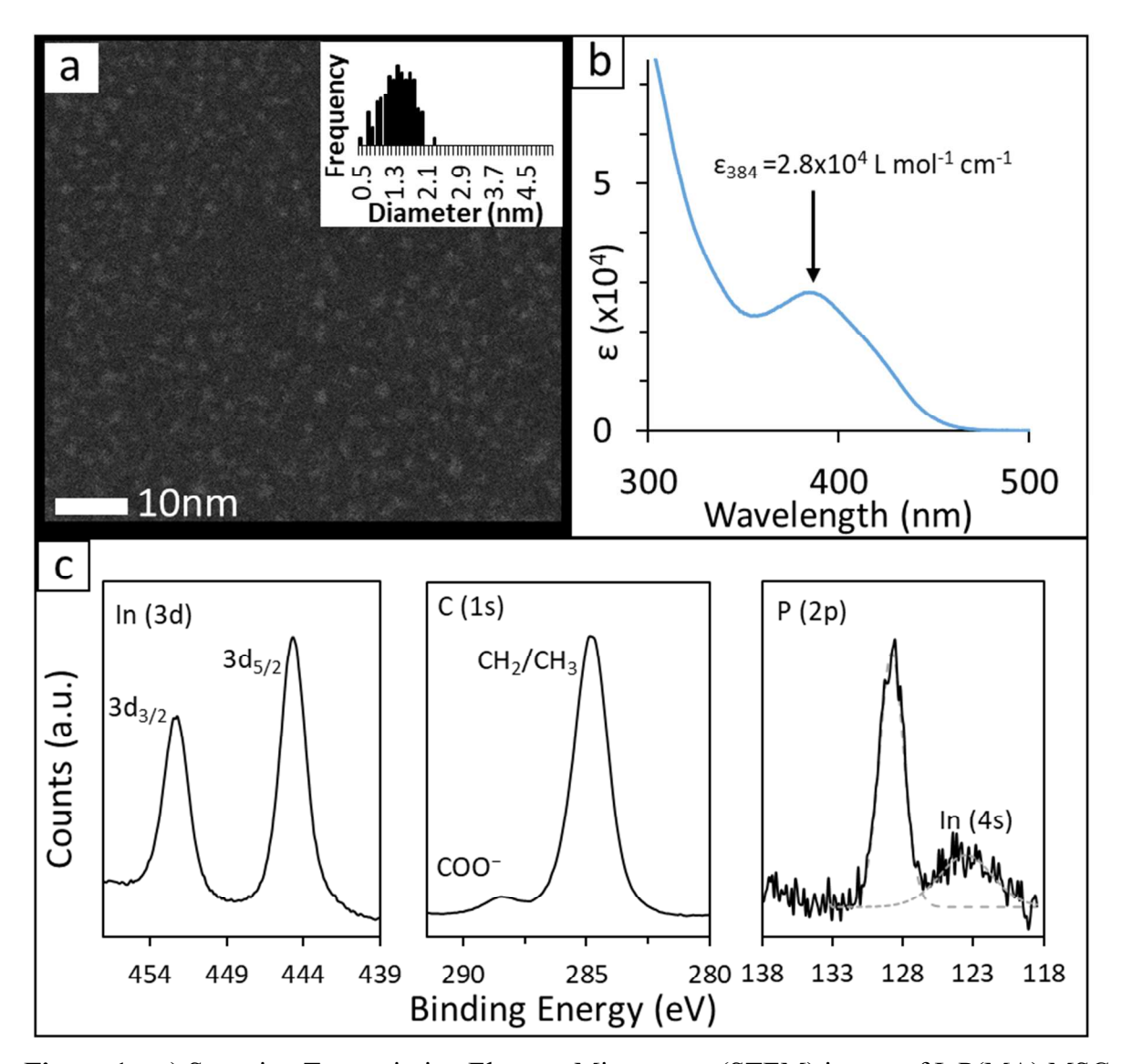


Figure 1 – a) Scanning Transmission Electron Microscope (STEM) image of InP(MA) MSCs. The size distribution histogram (inset) reveals an average MSC diameter of 1.3 nm with a standard deviation SD of 0.37 nm based on the analysis of n > 200 MSCs; b) Absolute UV-Vis absorption spectrum of 6.6 μ M InP(MA) MSC solution showing a well-defined excitonic peak at 384 nm, and a shoulder at 420 nm. Extinction coefficient is given on y-axis.; c) XPS measurements of InP MSCs confirm the presence of indium and phosphorous and agree with the previously reported atomic formula of InP MSCs (In₃₇P₂₀).

UV-Vis Spectroscopy of InP MSCs - A combination of UV-Vis and ICP-MS measurements was used to determine the molar absorptivity (ε_{384}) of InP(MA) MSCs. The concentrations of InP(MA) MSC samples were determined by utilizing ICP-MS measurements to quantify indium content. Using the previously reported atomic formula of InP MSCs of In₃₇P₂₀¹⁷, we could accurately determine cluster concentration as moles/gram of dry InP(MA) MSC. ICP-MS was used to remove any false contributions to the sample weight that may come from incomplete washing of MSCs. As such, dry purified InP(MA) MSCs were carefully weighed and dispersed in hexanes in a volumetric flask to give absorbance values between 0.1 and 1. Since these were the same MSC batches analyzed by ICP-MS, we could therefore calculate InP(MA) MSC molarity. The extinction coefficient is derived from Beer's law $\varepsilon = \frac{A}{ch}$ where A = absorbance, c = concentration and b = path length of light (1cm in our cuvette). We determine the extinction coefficient at the exitonic peak (ε_{384}) to be 2.8 x10⁴ L mole⁻¹ cm⁻¹ with a relative SD of 4.4%. This absorptivity value agrees with the absorptivity value of $\varepsilon_{390\text{nm}} = 1.9 \times 10^4 \text{ L mole}^{-1} \text{ cm}^{-1}$ for phenyl acetate (PA) coated InP(PA) MSCs¹⁷. Figure 1b describes the wavelength dependence of the extinction coefficient, ε , of InP(MA) MSCs on a per particle basis. ε_{310} and ε_{350} on a per InP unit basis are often used to determine InP concentrations, since these values are often size independent, absorption at these wavelengths scales predictably with particle volume and the number of InP units in a particle. Talapin and Bawendi have provided ε_{310} and ε_{350} per InP unit of 5,135 and 3,700 L mole⁻¹ cm⁻¹, respectively. ^{28,29} Looking at ε per MSC (from **figure 1b**), and dividing by 20 (the number of neutral InP units per MSC), we calculate the per InP unit \$\epsilon_{310}\$ and ε_{350} to be 3,155 and 1,200 L mole⁻¹ cm⁻¹, respectively. These ε (per InP unit) deviate slightly from the ones reported by Talapin and Bawendi, but agree quite closely with 3,200 and 1,300 L mole⁻¹ cm⁻¹ determined by Cossairt for phenyl acetate coated InP MSCs. ¹⁹ A few comments on the discrepancies: Both Talapin and Bawendi used fully formed QD to calculate molar extinction values where the crystal structure is more similar to bulk zinc blend, compared to the altered crystal structure of InP MSC. 19 It appears that this deviation from bulk crystal structure also affects the extinction coefficient of the clusters by lowering it. Additionally, the absorption value at 350nm of our MSCs lies within the exitonic feature of the cluster, therefore it is not sizeindependent like one would see in larger particles.

InPZn QD growth from MSCs monitored using UV-Vis, Photoluminescence and Scanning Transmission Electron Microscopy (STEM) - The synthesis of InPZn QD from InP(MA) MSCs was monitored by STEM imaging to measure changes in QD diameter. STEM images in Figure 2a (zinc: indium in the reaction mixture of 200%) and Figure 2b (zinc free, ie 0%) show that adding zinc stearate to the hot solvent before injection, while keeping all other reaction conditions identical, causes a significant restriction to QD crystal growth. InPZn QD (zinc : indium ratio of 200% in the reaction mixture) average 2.1 nm in diameter with a standard deviation SD = 0.49 nm (Figure 2a), while zinc free InP QD average 3.1 nm in diameter with SD = 0.54 nm (Figure 2b). UV-Vis spectroscopy (Figures 2c and 2d) shows a red-shift in the absorption peak as the QD grow, consistent with quantum confined excitons. The zinc free 3.1 nm InP QD have an absorption maximum at 553 nm (2.24 eV) (Figure 2d). This result is in excellent agreement with previous studies by Micic et. al. and Talapin et.al., who reported energy bandgaps of 2.2 eV and 2.19 eV for 3 nm InP QD. 28, 30 The InPZn QD (Figure 2c) have an absorption peak at 455 nm. For the InPZn/ZnS OD prepared from InP(MA) MSCs, a plot describing the emission peak position in energy units (eV) of InPZn QD vs the indium : zinc ratio in the reaction mixture is shown in **Figure S2**. An inflection point at zinc: indium ratio of 25% is observed. This could be attributed to a combination of two mechanisms that affect the emission peak wavelength of InPZn QD. The blue shift of the InPZn QD with increasing zinc: indium ratio in the reaction mixture used to form the InPZn QD from InP MSCs is attributed in part to the inclusion of zinc into the InP QD to possibly form and InPZn alloy QD, and to a steric effect in the presence of zinc stearate which restricts InPZn QD crystal growth. Regardless of the exact InPZn QD structure, adding zinc stearate to the reaction mixture provides a simple and predictable way to tune the QD size and emission color over a broad spectral range.

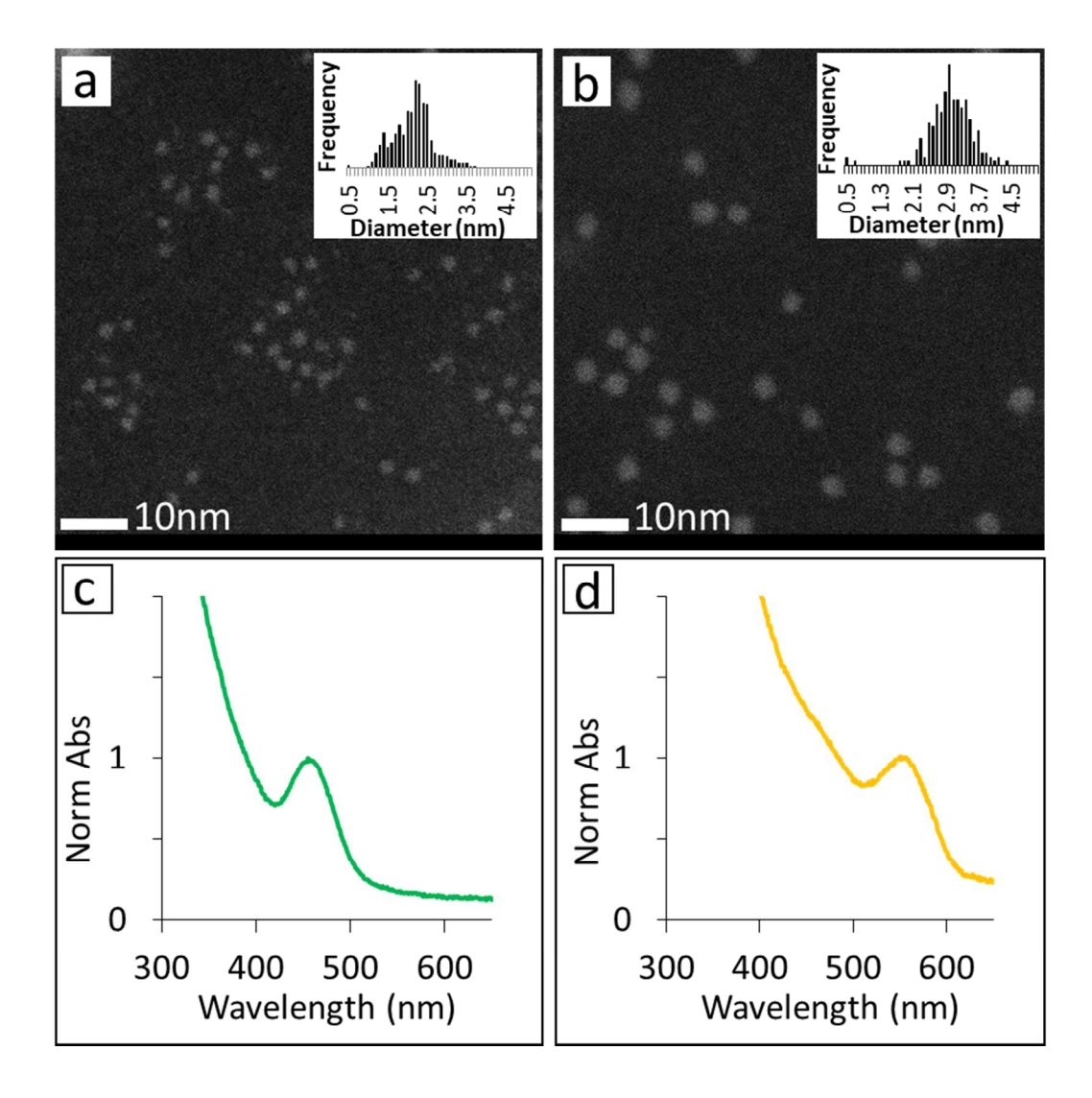


Figure 2 – a, b) STEM images of InPZn QD (zinc : indium ratio of 200% in the reaction mixture) and InP QD (zinc free reaction mixture). Histograms showing the size distributions of the resulting QD are shown in insets; c, d) UV-Vis spectra of InPZn QD (zinc : indium ratio of 200% in the reaction mixture) and InP QD (zinc free reaction mixture). The STEM images and UV-Vis spectra show that adding zinc stearate to the reaction mixture used to form InP QD from InP MSCs leads to the formation of zinc-containing InPZn QD which are smaller and have a shorter excitonic peak wavelength than zinc free InP QD.

Controlling InP OD Size and Emission Peak wavelength using Zinc Stearate - An important discovery in our work is that the inclusion of zinc stearate in the hot injection step produces highly emissive QD with narrow emission peaks after shelling, and provides excellent control over the emission peak wavelength, λ_{max} . The ability to produce luminescent QD with tunable emission colors is a defining characteristic of luminescent semiconductor QD. This allows the OD emission color to be tuned for specific applications with strict requirements, such as multiplexed cellular probes, Forster Resonance Energy Transfer (FRET) probes, and electronic displays. 19,20 To isolate the effect of zinc stearate, we varied the amount of zinc in the hot reaction mixture over a wide range of concentrations. 100 mg InP(MA) MSCs (6 umoles MSCs = 225 µmoles In³⁺) samples were used in each reaction, while the zinc: indium molar ratio was varied between 0% and 200% (0 to 450 µmoles zinc stearate). All other reaction conditions including solvent volume and reaction temperature and time were kept the same. The emission spectra of InPZn/ZnS core/shell QD with varying amounts of zinc in the reaction mixture are shown in Figure 3. Varying the amount of zinc in the reaction mixture from 0 to 200% results in tunable emission peaks of InPZn/ZnS QD over the blue-green to yellow-orange ends of the visible spectrum. **Table 2** shows the emission peak wavelength λ_{max} (nm), peak Full Width at Half Maximum (FWHM) in wavelength (nm) and energy (eV) units, and emission quantum yield (Φ_{PL}) of the InPZn/ZnS QD shown in **Figure 3**. The FWHM and Φ_{PL} change only slightly over this spectral window. The average FWHM of the InPZn/ZnS QD is 50 nm (2.2 eV) with a relative SD of 3.3%. The average Φ_{PL} of the InPZn/ZnS QD is 48% with a relative SD of 6%. This is an improvement in InP QD synthesis, since most methods to tune the emission peaks of luminescent QD by varying their size, require adjusting multiple reagent concentrations and/or temperature to yield optimal results with respect to emission peak widths and quantum yield. It should be noted that the inclusion of sulfur in the reaction mixture used to form the InP QD from InP MSCs had a much smaller effect on the QD emission spectra compared to the effect of zinc stearate (data not shown). Only a slight shift in the emission peak was observed when increasing levels of 1-dodecanethiol to realize a sulfur: indium ratio of up to 10% were included in the reaction mixture. Adding larger amounts of sulfur (> 10% sulfur: indium) resulted in emission peak broadening. Furthermore, 1-dodecanethiol quickly degraded the excitonic peak of InP(MA) MSCs at room temperature, indicating that the sulfur ligands destabilize the InP MSCs similarly to the previously reported effect of amines on InP MSCs.^{6,9} This excludes the possibility of

adding 1-dodecanethiol directly to the InP(MA) MSC solution prior to injection. It must be added after the formation of InPZn QD as a shell precursor.

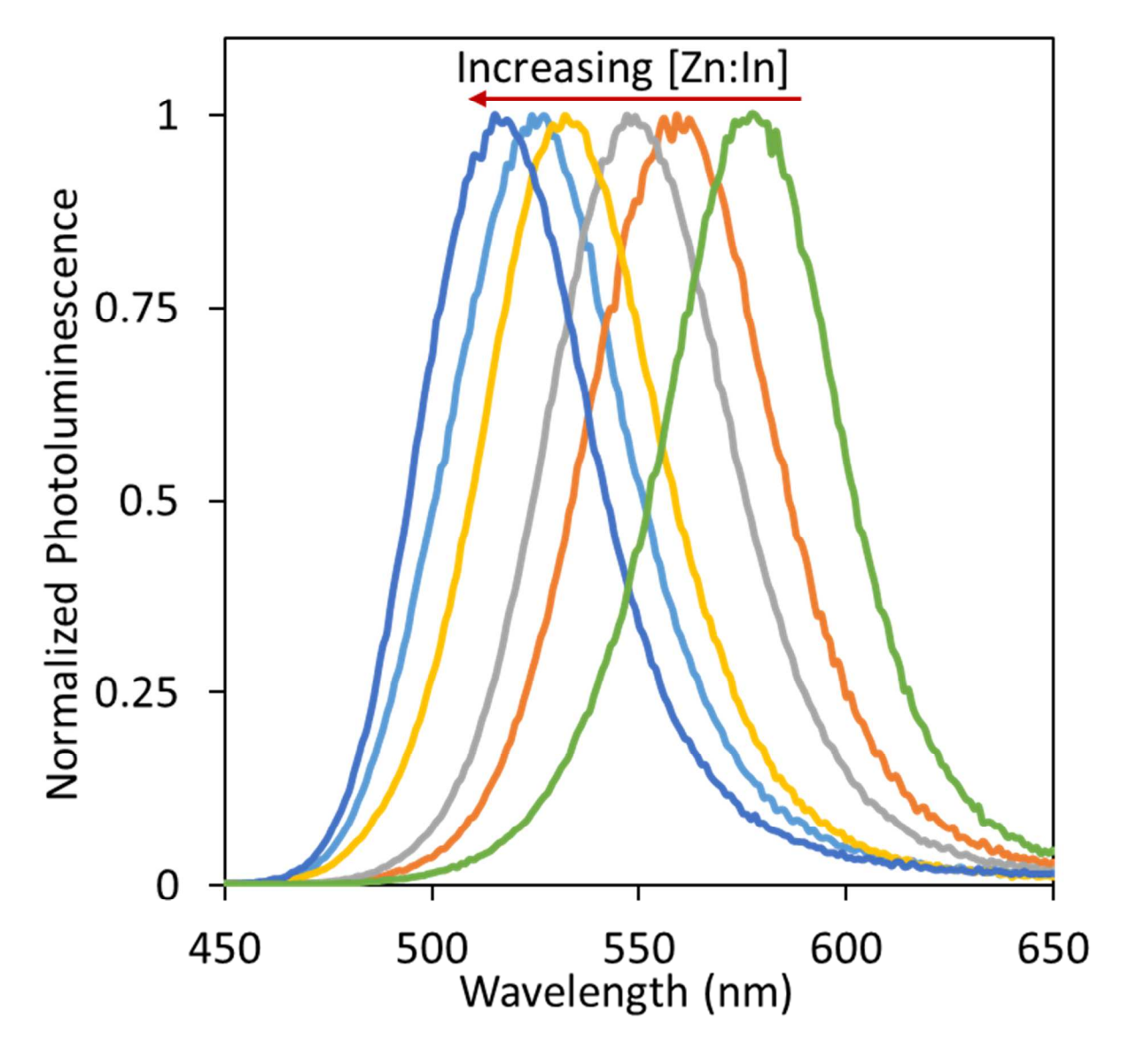


Figure 3 – Normalized photoluminescence (PL) spectra of InPZn/ZnS core/shell QD with various zinc : indium ratios in the reaction mixture. From left to right, zinc equals 200%, 100%, 50%, 25%, 10% and 0%. Narrow and tunable emission peaks are observed between 500 and 600 nm.

Zn:In	PL λ _{max}	FWHM (λ)	FWHM (eV)	$\Phi_{ t PL}$
200%	515nm	47nm	0.217	47% ±3%
100%	524nm	50nm	0.225	49% ±3%
50%	532nm	50nm	0.218	46% ±1%
25%	547nm	52nm	0.214	52% ±2%
10%	559nm	52nm	0.206	47% ±3%
0%	577nm	50nm	0.187	45% ±4%

Table 2 – Properties of InPZn/ZnS QD for different zinc : indium (Zn:In) ratio in the reaction mixture: photoluminescence (PL) peak wavelength, emission peak full width at half maximum (FWHM) in wavelength (λ) and energy units (eV), and photoluminescence quantum yield, Φ_{PL} .

Thermal and Chemical Stability Studies of InPZn core and InPZn/ZnS core/shell OD - As described above, forming InPZn/ZnS QD from InP MSCs results in excellent photophysical properties including high emission quantum yield and narrow, symmetric, and tunable emission peaks. The QD maintain their optical properties when stored in the dark in the presence of excess stabilizing ligands. However, any optical nanomaterial offered as a replacement to CdSe QD should also provide long term thermal and chemical stability under operating conditions in the absence of excess ligands. We therefore compared the long term thermal and chemical stability of InPZnS alloy QD made from molecular precursors (P(TMS)₃ and indium myristate) and InPZn OD made from MSCs to the thermal and chemical stability of CdSe OD towards oxidation. Figure 4 shows UV-Vis absorption spectra of CdSe and InPZn QD over 48 hours once excess stabilizing ligands are removed. The QD were suspended in toluene and kept at room temperature in a capped cuvette. No effort was made to exclude oxygen from the QD solution. Figures 4a and 4d describe the chemical stability of CdSe QD towards oxidation when stored in room light (Figure 4a) and in the dark (Figure 4d). When stored in room light (Figure 4a), a decrease in the high energy absorption peak of CdSe QD at 410 nm is observed. However, no significant change in the band edge absorption peak at 520 nm is observed. When stored in the dark, no significant changes in the absorption peaks of CdSe QD are observed (**Figure 4c**). Figures 4b and 4e follow the chemical stability of InPZnS QD made from molecular precursors (InPZn MP OD) when stored in room light (**Figure 4b**) and in the dark (**Figure 4e**). A significant decrease in InPZnS MP QD band edge absorption along with a blue shift are observed over 28 hours when the QD are stored in room light (**Figure 4b**). The absorption spectrum stabilizes and remains almost constant over longer periods of observation up to 48 hours, possibly due to consumption of oxygen in the headspace of the cuvette. The QD degradation is significantly lower when the InPZnS MP QD are stored in the dark (Figure 4e). Figures 4c and 4f show that similar degradation results are obtained for InPZn QD made from MSCs (InPZn MSC QD). The UV-Vis absorption results clearly show that InPZn-based QD degrade faster than CdSe QD regardless of the synthesis technique used to prepare them, particularly in the presence of light. CdSe QD degradation result in a loss of absorption peaks associated with higher energy transitions, around 410nm. The band edge transition responsible for photoemission remain relatively sharp, blue shifting slightly. In contrast, the InP-based QD have their band edge peaks broaden over time. These results indicate that InPZn InPZnS QD are clearly more sensitive to photooxidation than CdSe QD.

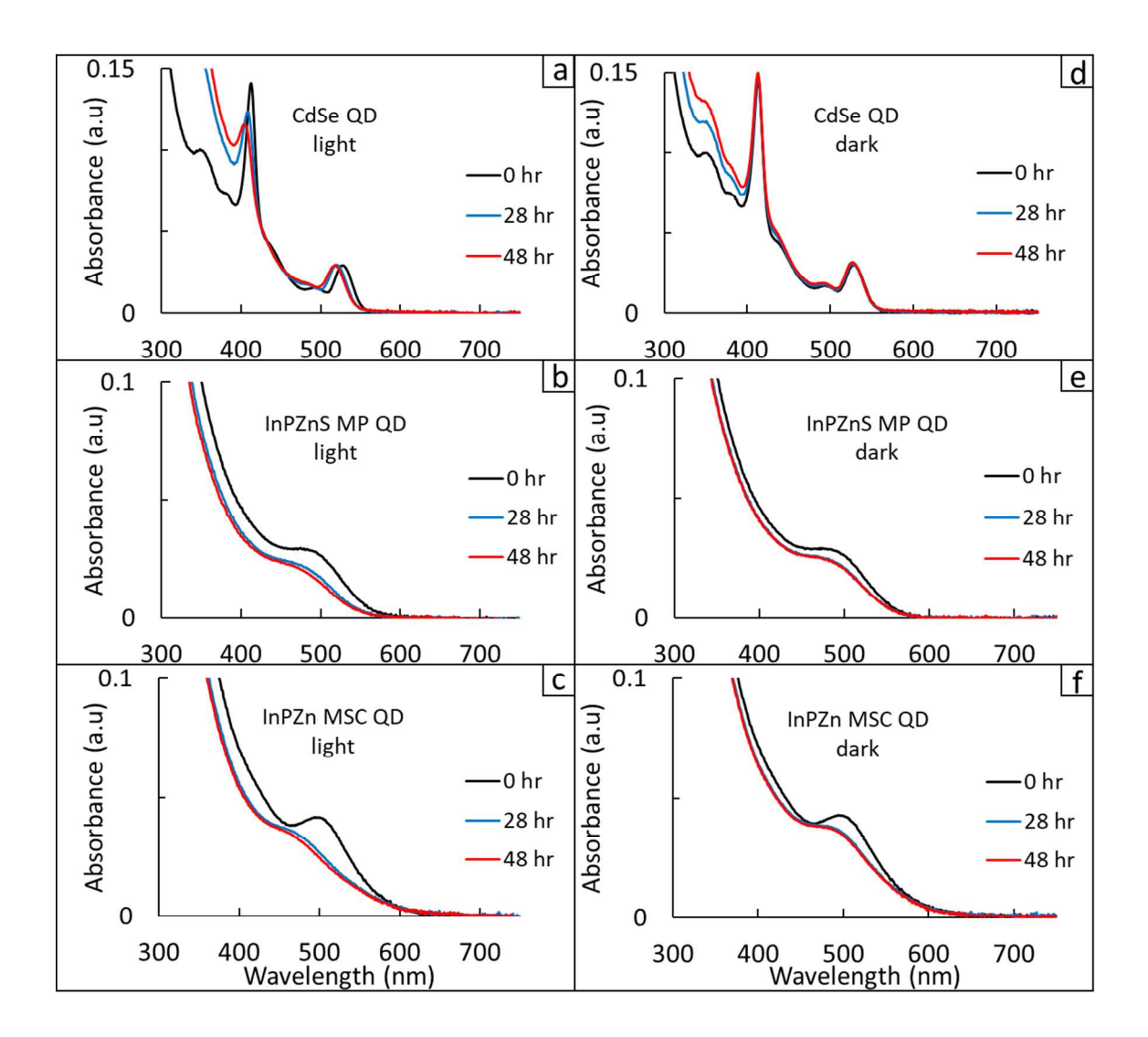


Figure 4 - Degradation of QD at room temperature when exposed to light (a-c) and when kept in dark (d-f)

Since luminescent OD are often used in devices with higher operating temperatures then room temperature, it is also important to evaluate the thermal stability of InP-based QD at elevated temperature. We chose 90°C as a representative case. The results of the thermal stability measurements of CdSe QD and InP-based QD made from MSCs and from molecular precursors at 90°C are shown in Figure 5(a-c) for air-containing QD solutions, and Figure 5(b-d) for nitrogenated (oxygen free) OD solutions. Figure 5 shows a significantly higher thermal degradation rate of CdSe and InP-based QD (compared to results shown in Figure 4) when incubated in air-containing solutions at elevated temperature. Figure 5a shows that CdSe QD maintain their sharp excitonic features when incubated in air-containing solution at 90°C for one hour. Only a slight blue shift in the emission peak of CdSe QD is observed under these conditions. Figure 5b and 5c show a higher degradation rate for InP-based QD made from molecular precursors (figure 5b) and from MSCs (figure 5c) under the same conditions. The rapid InP-based QD degradation, which occurs within 1 hour of incubation at elevated temperature might be attributed to oxidation of dangling surface phosphide bonds. Figure 5(b-d) demonstrates the effect of removing oxygen on the QD degradation rate under conditions of elevated temperature. A significant increase in thermal stability is seen for all QD types. It is also interesting to note that a new higher energy excitonic feature emerge (~313nm) as the InPbased QD are purged with nitrogen. Adsorbed oxygen seems to affect this peak more strongly. It is fair to conclude, based on these thermal stability experiments, that under ambient conditions, InP-based QD are significantly less stable towards oxidation than CdSe QD. The rate of QD oxidation increases with temperature and decreases with the elimination of oxygen for all QD types. In contrast, oxidation of CdSe QD when incubated for one hour at elevated temperature impacts higher energy excitonic features with minimal impact of the band edge excitonic feature. This results in the preservation of the emission properties of CdSe QD when exposed to heat in the presence of oxygen.

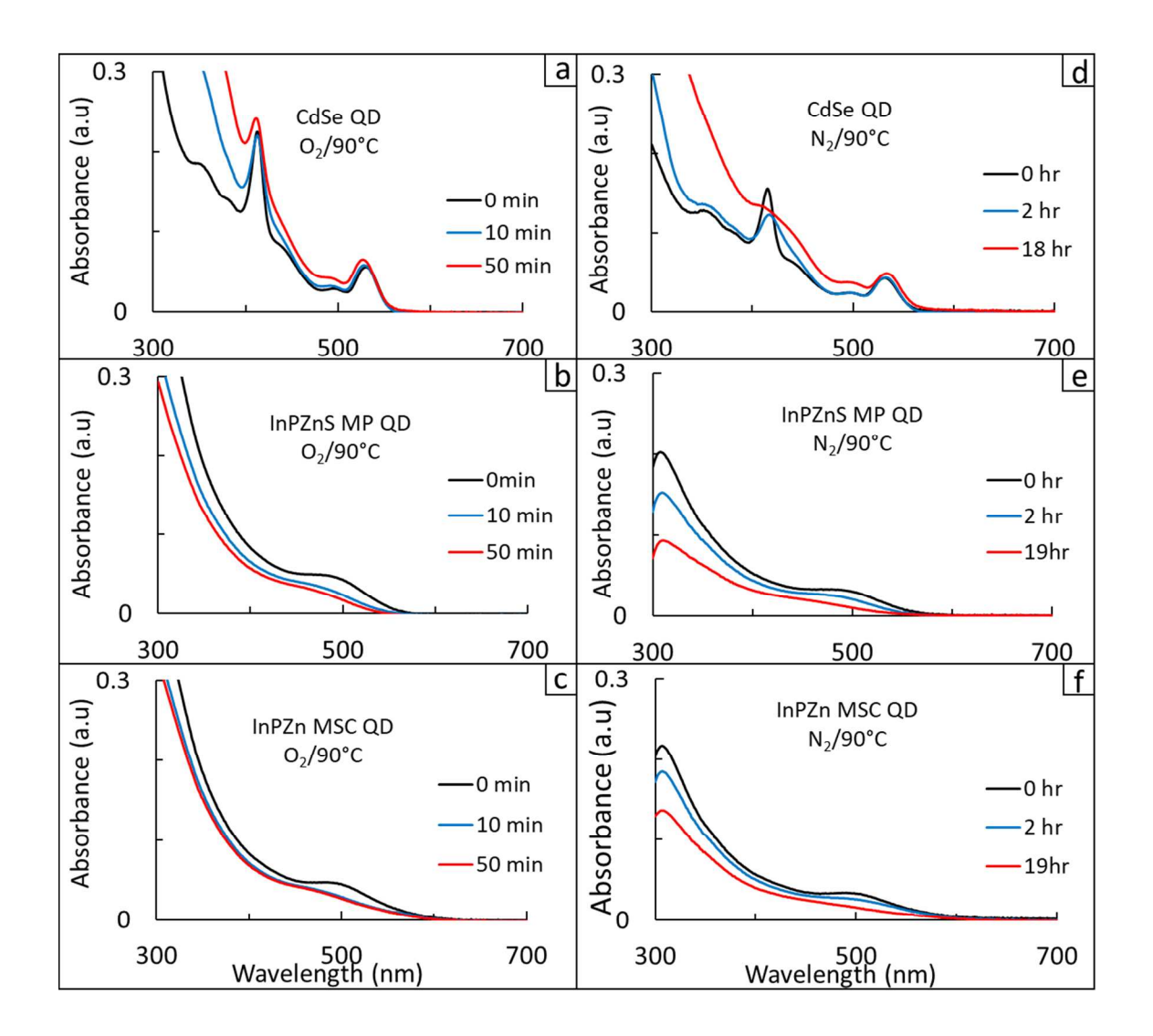


Figure 5 - Degradation of QD cores at 90°C monitored by UV-Vis absorbance. With air (a-c) and under nitrogen (d-f). Please note the different time scales for O_2 vs N_2 conditions.

Growing a higher bandgap material over the OD cores has been used effectively to passivate the QD cores to maximize their photoluminescence and protect the QD from chemical degradation due to interaction with oxygen and other molecules in their storage solutions. InPbased QD were coated with ZnS using zinc stearate and 1-dodecanethiol. This method was chosen since it represents the most commonly reported one in the literature and is described in the materials and methods section. Figure 6 describes the impact of coating CdSe and InP-based QD with a ZnS shell on their UV-Vis and luminescence properties. Figure 6(a-c) shows that coating CdSe QD (figure 6a), and InPZnS QD made from molecular precursors (figure 6b), and InPZn OD made from MSCs (figure 6c) significantly decreases the degradation rate of all OD types when suspended in air-containing solutions at room temperature. The excitonic features of CdSe QD remain highly stable for 14 days under these conditions. Some reduction in QD absorption is observed for InP-based QD (figure 6b and 6c), but their excitonic features are largely preserved regardless of whether they are prepared from molecular precursors or MSCs. Monitoring the photoluminescence spectra of the same samples shows a slight decrease in photoluminescence of CdSe/ZnS QD during the first day of storage, probably due to the release of loosely bound surface atoms to the solution. As seen in **Figure 6d**, the CdSe/ZnS photoluminescence remains stable for 14 days after the initial loss of photoluminescence. In contrast, a much larger loss of about 80% in the photoluminescence of the InPZnS/ZnS made from molecular precursors (Figure 6e) and InPZn/ZnS QD made from InP MSCs (Figure 6f) are observed during the first day. This is while their UV-Vis spectra remain largely unchanged. This significant reduction in QD photoluminescence is attributed to poor quality of the ZnS shell as it grows on the III-V QD cores compared to the high quality of ZnS shell of II-VI CdSe/ZnS QD. The alloying approach is proposed to overcome poor passivation of core defects with the ZnS shell, which it does in terms of increasing photoluminescence in pristine samples. Once diluted in working concentrations, however, it seems that simply alloying with zinc and sulfur is not sufficient to provide QD that are structurally stable as the CdSe/ZnS core/shell QD. Additionally, zinc stearate and 1-dodecanethiol seem to be poor choices for shelling precursors. More reactive sulfur precursors, such as TOP-S would be a better choice.

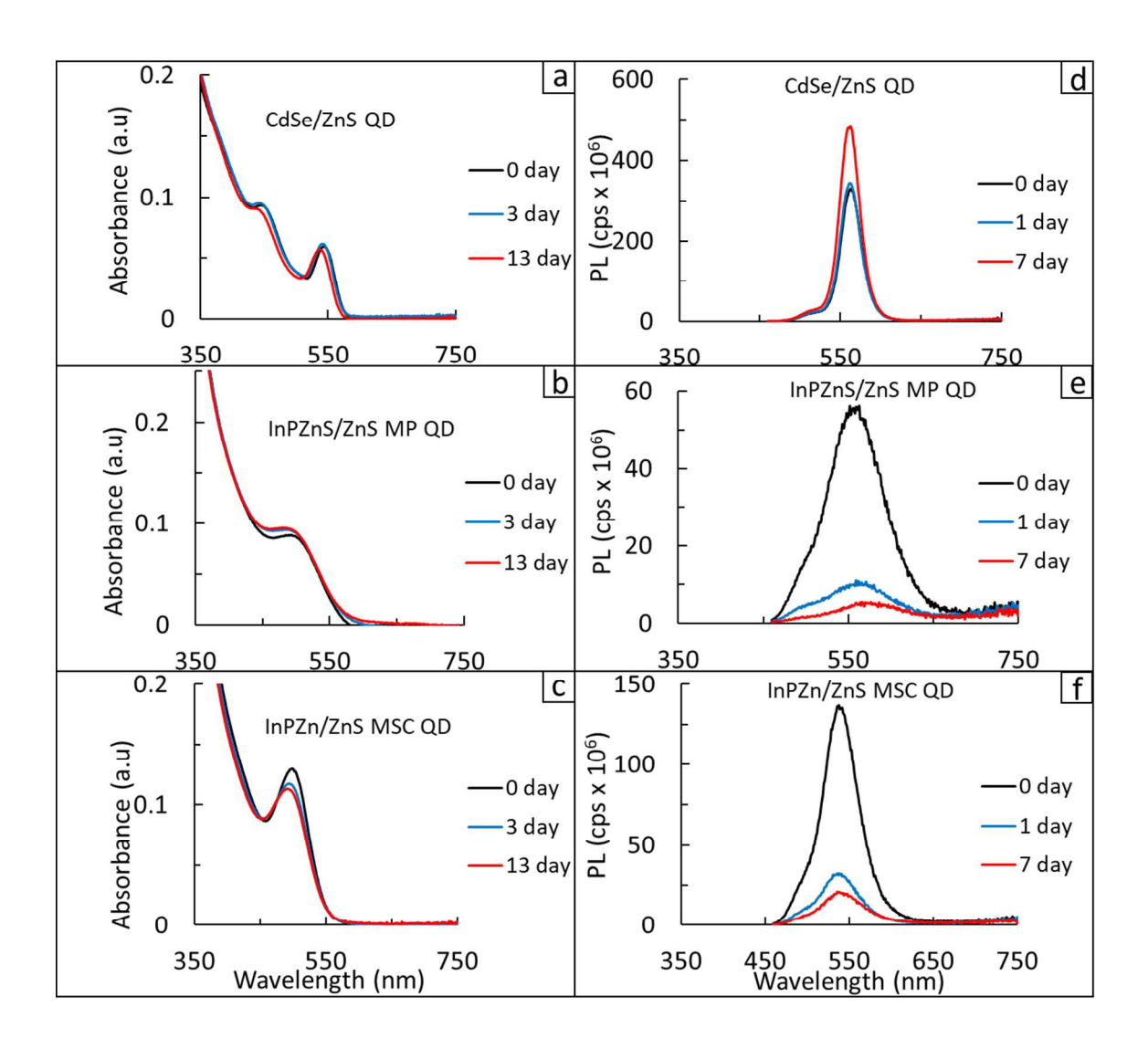


Figure 6 - Degradation of core/shell QD at room temperature followed by UV-Vis (a-c) and photoluminescence (d-f)

SUMMARY

We demonstrated a synthesis route for the formation of highly luminescent InPZn/ZnS QD with good optical properties. The synthesis of InPZn/ZnS QD from InP MSCs can be accomplished in a few hours with no exposure to toxic, pyrophoric reagents. This removes a major obstacle for using luminescent InP OD as an alternative to cadmium-containing luminescent OD, like CdSe QD in a broad range of applications While the spectroscopic properties of InP and InPZn/ZnS QD are promising, chemical degradation measurements reveal that InP QD exhibit lower stability towards oxidation than CdSe OD under conditions of elevated temperature in the presence of oxygen. The use of InP MSCs as a single source reactant, which greatly simplifies the synthesis of InP QD does not impact their susceptibility to oxidation. As expected, coating InP QD with a higher bandgap energy ZnS shell slows the thermal degradation of InP QD considerably. However, InPZn/ZnS QD do not maintain their luminescence properties once excess ligands used to stabilize the OD are removed. This effect is accelerated when the OD are exposed to light, heat and oxygen. This might not prove problematic in applications, like QDpolymer film composites where the presence of oxygen could be minimized or even eliminated. However, further advances in shelling procedures are required to enable the formation of stable InP-based core-shell QD, which are suitable for applications in air-containing solutions at room temperature and under conditions of elevated temperature.

ASSOCIATED CONTENT

Supporting Information

High Resolution Transmission Electron Microscopy (HRTEM) of InPZn Quantum Dots (figure S1), calculation of extinction coefficient for InP(MA) MSCs, plot of peak energy for different [Zn]:[In] ratios (figure S2)

ACKNOWLEDGMENTS

This work was supported primarily by the National Science Foundation Center for Chemical Innovation (CCI) program Award CHE-1503408 for the Center for Sustainable Nanotechnology. High resolution electron microscopy studies of InP MSCs and InPZn/ZnS QD were supported by NSF Award CHE-1506995. A supplemental fellowship support for Richard Brown's graduate assistantship was provided by the UMBC Chemistry Biology Interface program, which is supported by an NIH training grant: NIH-T32-GM066706. The authors thank Dr. Alline Myers of the NIST Center for Nanoscale Science and Technology for her assistance with TEM imaging.

REFERENCES

- 1. Li, L.; Reiss, P., One-pot synthesis of highly luminescent InP/ZnS nanocrystals without precursor injection. *Journal of the American Chemical Society* **2008**, *130* (35), 11588.
- 2. Kim, T.; Kim, S.; Kang, M., Large-Scale Synthesis of InPZnS Alloy Quantum Dots with Dodecanethiol as a Composition Controller. *Journal of Physical Chemistry Letters* **2012**, *3* (2), 214-218.
- 3. Xi, L.; Cho, D. Y.; Duchamp, M.; Boothroyd, C. B.; Lek, J. Y.; Besmehn, A.; Waser, R.; Lam, Y. M.; Kardynal, B., Understanding the role of single molecular ZnS precursors in the synthesis of In(Zn)P/ZnS nanocrystals. *ACS Appl Mater Interfaces* **2014**, *6* (20), 18233-42.
- 4. Altintas, Y.; Talpur, M.; Unlu, M.; Mutlugun, E., Highly Efficient Cd-Free Alloyed Core/Shell Quantum Dots with Optimized Precursor Concentrations. *Journal of Physical Chemistry C* **2016**, *120* (14), 7885-7892.
- 5. Mordvinova, N. E.; Vinokurov, A. A.; Lebedev, O. I.; Kuznetsova, T. A.; Dorofeev, S. G., Addition of Zn during the phosphine-based synthesis of indium phospide quantum dots: doping and surface passivation. *Beilstein J Nanotechnol* **2015**, *6*, 1237-46.
- 6. Gary, D.; Terban, M.; Billinge, S.; Cossairt, B., Two-Step Nucleation and Growth of InP Quantum Dots via Magic-Sized Cluster Intermediates. *Chemistry of Materials* **2015**, *27* (4), 1432-1441.
- 7. Adam, S.; Talapin, D.; Borchert, H.; Lobo, A.; McGinley, C.; de Castro, A.; Haase, M.; Weller, H.; Moller, T., The effect of nanocrystal surface structure on the luminescence properties: Photoemission study of HF-etched InP nanocrystals. *Journal of Chemical Physics* **2005**, *123* (8).
- 8. Haubold, S.; Haase, M.; Kornowski, A.; Weller, H., Strongly luminescent InP/ZnS core-shell nanoparticles. *Chemphyschem* **2001**, *2* (5), 331-334.
- 9. Xie, R.; Battaglia, D.; Peng, X., Colloidal InP nanocrystals as efficient emitters covering blue to near-infrared. *J Am Chem Soc* **2007**, *129* (50), 15432-3.
- 10. Xu, S.; Ziegler, J.; Nann, T., Rapid synthesis of highly luminescent InP and InP/ZnS nanocrystals. *Journal of Materials Chemistry* **2008**, *18* (23), 2653-2656.
- 11. Harris, D. K.; Bawendi, M. G., Improved precursor chemistry for the synthesis of III-V quantum dots. *J Am Chem Soc* **2012**, *134* (50), 20211-3.
- 12. Gary, D.; Glassy, B.; Cossairt, B., Investigation of Indium Phosphide Quantum Dot Nucleation and Growth Utilizing Triarylsilylphosphine Precursors. *Chemistry of Materials* **2014**, *26* (4), 1734-1744.
- 13. Tessier, M.; Dupont, D.; De Nolf, K.; De Roo, J.; Hens, Z., Economic and Size-Tunable Synthesis of InP/ZnE (E = S, Se) Colloidal Quantum Dots. *Chemistry of Materials* **2015**, *27* (13), 4893-4898.
- 14. Pietra, F.; Trizio, L. D.; Hoekstra, A. W.; Renaud, N.; Prato, M.; Grozema, F. C.; Baesjou, P. J.; Koole, R.; Manna, L.; Houtepen, A. J., Tuning the Lattice Parameter of InxZnyP for Highly Luminescent Lattice-Matched Core/Shell Quantum Dots. *ACS Nano* **2016**, *10*, 4754-4762.
- 15. Ramasamy, P.; Ko, K.-J.; Kang, J.-W.; Lee, J.-S., Two-Step "Seed-Mediated" Synthetic Approach to Colloidal Indium Phosphide Quantum Dots with High-Purity Photo- and Electroluminescence *Chem. Mater.* **2018**, *30*, 3643–3647.
- 16. Wang, Y.; Liu, Y. H.; Zhang, Y.; Wang, F.; Kowalski, P. J.; Rohrs, H. W.; Loomis, R. A.; Gross, M. L.; Buhro, W. E., Isolation of the magic-size CdSe nanoclusters [(CdSe)13(n-octylamine)13] and [(CdSe)13(oleylamine)13]. *Angew Chem Int Ed Engl* **2012**, *51* (25), 6154-7.
- 17. Xie, R.; Li, Z.; Peng, X., Nucleation Kinetics vs Chemical Kinetics in the Initial Formation of Semiconductor Nanocrystals. *Journal of the American Chemical Society* **2009**, *131* (42), 15457-15466.
- 18. Friedfeld, M.; Stein, J.; Cossairt, B., Main-Group-Semiconductor Cluster Molecules as Synthetic Intermediates to Nanostructures. *Inorganic Chemistry* **2017**, *56* (15), 8689-8697.

- 19. Gary, D.; Flowers, S.; Kaminsky, W.; Petrone, A.; Li, X.; Cossairt, B., Single-Crystal and Electronic Structure of a 1.3 nm Indium Phosphide Nanocluster. *Journal of the American Chemical Society* **2016**, *138* (5), 1510-1513.
- 20. Jang, E.; Jo, J.; Kim, M.; Yoon, S.; Lim, S.; Kim, J.; Yang, H., Near-complete photoluminescence retention and improved stability of InP quantum dots after silica embedding for their application to on-chip-packaged light-emitting diodes. *Rsc Advances* **2018**, *8* (18), 10057-10063.
- 21. Cho, S.; Kwag, J.; Jeong, S.; Baek, Y.; Kim, S., Highly Fluorescent and Stable Quantum Dot-Polymer-Layered Double Hydroxide Composites. *Chemistry of Materials* **2013**, *25*, 1071-1077.
- 22. Ramasamy, P.; Kim, N.; Kang, Y.; Ramirez, O.; Lee, J., Tunable, Bright, and Narrow-Band Luminescence from Colloidal Indium Phosphide Quantum Dots. *Chemistry of Materials* **2017**, *29* (16), 6893-6899.
- 23. Lim, J.; Bae, W.; Lee, D.; Nam, M.; Jung, J.; Lee, C.; Char, K.; Lee, S., InP@ZnSeS, Core@Composition Gradient Shell Quantum Dots with Enhanced Stability. *Chemistry of Materials* **2011**, *23* (20), 4459-4463.
- 24. Pietra, F.; Kirkwood, N.; De Trizio, L.; Hoekstra, A.; Kleibergen, L.; Renaud, N.; Koole, R.; Baesjou, P.; Manna, L.; Houtepen, A., Ga for Zn Cation Exchange Allows for Highly Luminescent and Photostable InZnP-Based Quantum Dots. *Chemistry of Materials* **2017**, *29* (12), 5192-5199.
- 25. Zhang, J.; Li, R.; Sun, W.; Wang, Q.; Miao, X.; Zhang, D., Temporal evolutions of the photoluminescence quantum yields of colloidal InP, InAs and their core/shell nanocrystals. *Journal of Material Chemistry C* **2014**, *2* (22).
- 26. Jasieniak, J.; Smith, L.; van Embden, J.; Mulvaney, P.; Califano, M., Re-examination of the Size-Dependent Absorption Properties of CdSe Quantum Dots. *Journal of Physical Chemistry C* **2009**, *113* (45), 19468-19474.
- 27. NIST X-ray Photoelectron Spectroscopy Database. National Institute of Standards and Technology, Gaithersburg, 2012; Vol. Version 4.1.
- 28. Talapin, D. V., Experimental and theoretical studies on the formation of highly luminescent II-VI, III-V and core-shell semiconductor nanocrystals University of Hamburg, 2002; pp 1-149.
- 29. Xie, L.; Shen, Y.; Franke, D.; Sebastian, V.; Bawendi, M.; Jensen, K., Characterization of Indium Phosphide Quantum Dot Growth Intermediates Using MALDI-TOF Mass Spectrometry. *Journal of the American Chemical Society* **2016**, *138* (41), 13469-13472.
- 30. Micic, O.; Cheong, H.; Fu, H.; Zunger, A.; Sprague, J.; Mascarenhas, A.; Nozik, A., Size-dependent spectroscopy of InP quantum dots. *Journal of Physical Chemistry B* **1997**, *101* (25), 4904-4912.